Pramāṇa, Vol. 20, No. 3, March 1983, pp. 183–192. © Printed in India.

Raman scattering study of $LiKSO_4$—phases II and III

M L BANSAL, S K DEB, A P ROY and V C SAHNI
Nuclear Physics Division, Bhabha Atomic Research Centre,
Bombay 400 085, India

MS received 8 September 1982

Abstract. Detailed Raman scattering investigation of $LiKSO_4$ in phases II and III across the transition temperature $T_c \simeq 700$ K is reported. Abrupt change in frequency and line width of the external and internal modes have been observed. Analysis of the results suggests lithium positional disorder and sulphate orientational disorder in the high temperature phase (II). The results also throw some light on the existence of twin domains in the crystal.

Keywords. Raman scattering; $LiKSO_4$; phase transition; twinning; lithium positional disorder; sulphate orientational disorder.

1. Introduction

Light scattering has been used as an effective tool in investigating phase transitions in solids. Lithium potassium sulphate is known to be pyroelectric in phase III but not ferroelectric (Ando 1962). Further the ionic conductivity of $LiKSO_4$ (Ando 1962) displays an abrupt increase at the transition temperature ($T_c \simeq 700$K). The above features can be related to the orientational configuration of SO_4^{2-} and positional disorder of Li^+. The temperature dependent study of the dynamics of $LiKSO_4$ presented in this paper throws some light on these aspects.

Several techniques have been used to investigate the physical properties of lithium potassium sulphate. These include (i) structure by x-ray and neutron diffraction (Chung and Hahn 1972; Bhakay *et al* 1981 a) (ii) dynamics by Raman and IR (Mathieu *et al* 1955, Hiraishi *et al* 1976, Bansal *et al* 1979, 1980 a (iii) thermal expansion (Ranga Prasad *et al* 1978; Sharma 1979) (iv) electrical conductivity (v) pyroelectricity and (vi) dielectric constant (Ando 1962; Breczewski *et al* 1981; Madhu and Narayanan 1981). On the basis of these investigations we enumerate the different phases as follows:*

$$\mathrm{I} \;\underset{}{\overset{\sim 940\mathrm{K}}{\longleftarrow}}\; \mathrm{II} \;\underset{\sim 685\mathrm{K}}{\overset{\sim 700\mathrm{K}}{\rightleftarrows}}\; \mathrm{III} \;\underset{\sim 201\mathrm{K}}{\overset{\sim 242\mathrm{K}}{\rightleftarrows}}\; \mathrm{IV} \;\underset{}{\overset{\sim 178\mathrm{K}}{\longleftarrow}}\; \mathrm{V}$$

The investigations of V-IV and IV-III phase transitions have already been reported by us (Bansal *et al* 1979, 1980 a). In this paper we shall confine ourselves mainly to

*Breczewski *et al* 1981 report anomalies in dielectric constant at 193 K and 257 K while heating. The values are higher by about 15° from the transition temperatures determined by us on the basis of Raman spectra. The transition temperatures as determined by preliminary DSC (Differential Scanning Calorimetry) runs in our laboratory are in close agreement with the Raman data.

Raman scattering study in the phases III and II across the transition temperature $T_c \simeq 700$K. The transition to phase II could not be established in our preliminary work at elevated temperatures which was reported earlier (Bansal *et al* 1980 b).

The crystal structure (Wyckoff 1965) in phase III (space group $P6_3$; bimolecular unit cell) is shown in figure 1. The coordinates of the atoms are given below (Bhakay 1981 b:)

K	: 0, 0, 0
S	: 1/3, 2/3, 0·2066
Li	: 1/3, 2/3, 0·8147
0(1)	: 1/3, 2/3, 0·0357
0(2)	: 0·3417, 0·9397, 0·2587

a=5·146, c=8·636 at 296 K.

Detailed structural data for phase II are not available; it is believed to have orthorhombic symmetry (Chung and Hahn 1972).

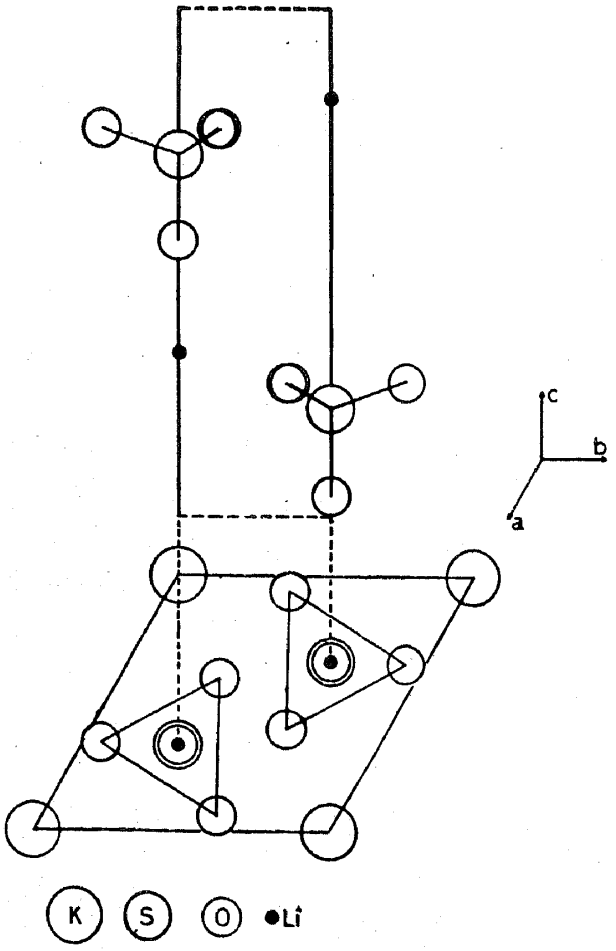

Figure 1. Crystal structure of $LiKSO_4$ in phase III.

2. Results

Polarized Raman spectra were recorded in a right-angled scattering geometry using a home-made 50 mW He-Cd laser (λ=4416 Å) and grating double monochromator with spectral bandpass of 3·5 cm^{-1}. The high temperature cell was made out of 'Syndanio' (compressed asbestos) with appropriate openings for incoming and outgoing beams. The crystal was held within a copper block such that contact was ensured on three faces. The temperature of the block was monitored using a chromel-alumel thermocouple and a proportional temperature controller was used to maintain it constant to within $\pm$ 0·5°C. The actual temperature of the crystal may be lower than that of the block. The spectra recorded above and below T_c are shown in figures 2-5.

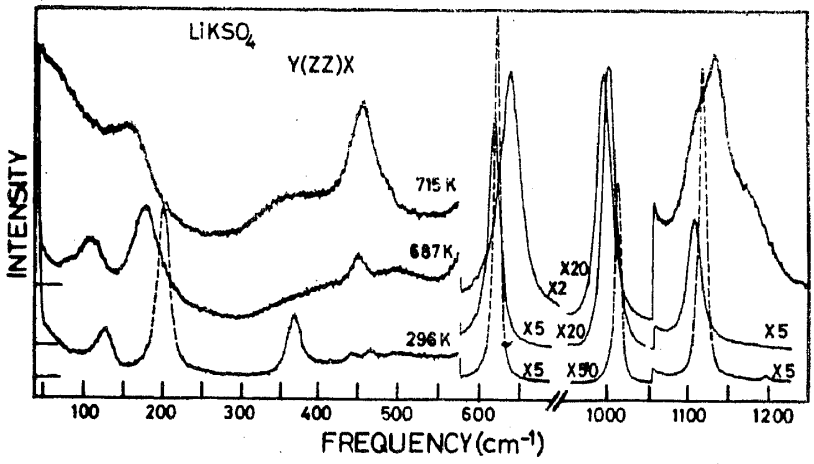

Figure 2. Raman spectra of $LiKSO_4$ at selected temperatures below and above T_c (= 700 K) in the Y(ZZ)X scattering configuration. In phase III, *i.e.* below T_c, these modes correspond to A(TO) symmetry (see table 1).

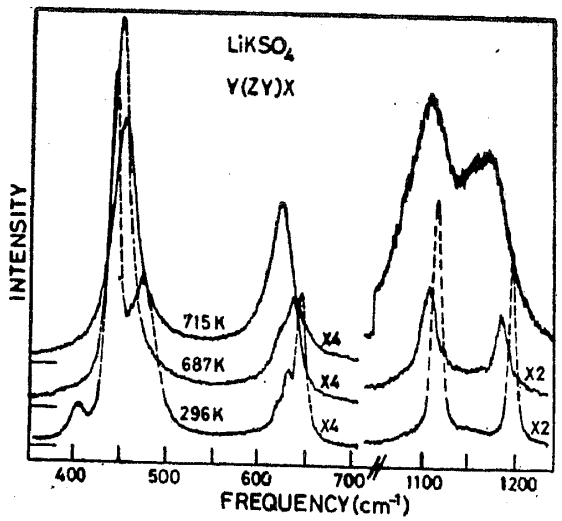

Figure 3. Raman spectra in the Y(ZY)X scattering geometry. In phase III, the modes correspond to either E_1(TO) or E_1(LO) symmetry (table 1).

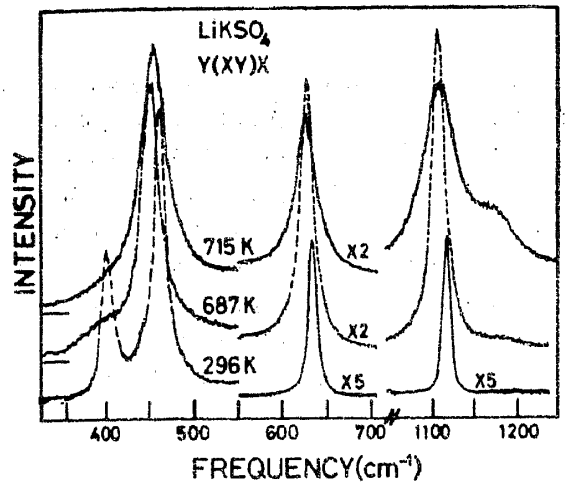

Figure 4. Raman spectra in the Y(XY)X geometry. In phase III, the modes correspond to E_2 symmetry (table 1).

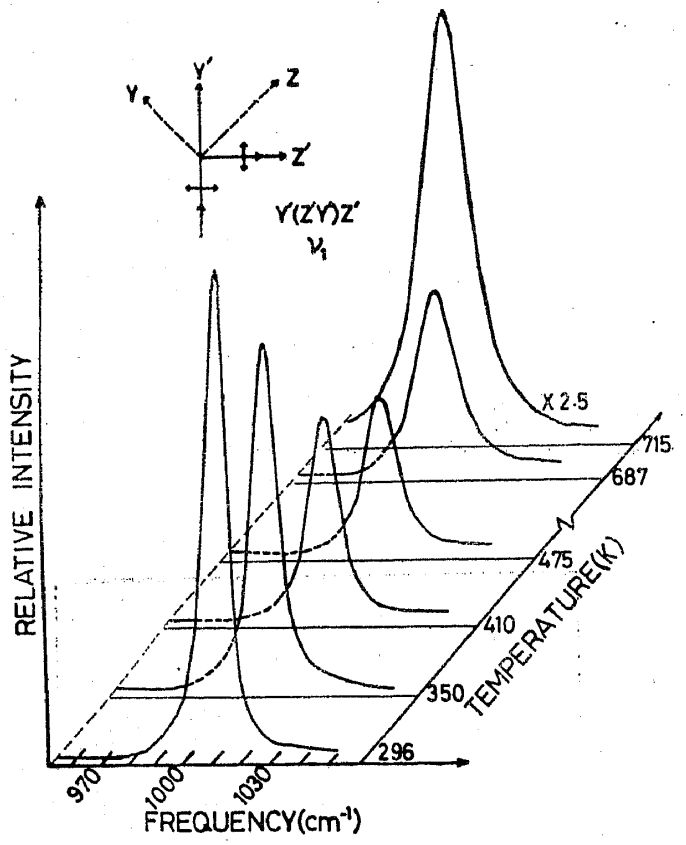

Figure 5. Intensity profiles of the ν_1 mode in an off-diagonal configuration as a function of temperature. Note the sudden increase in intensity above T_c; the 715 K profile is plotted on a compressed scale.

Porto's notation in identifying various scattering geometries has been followed; Z is taken along the crystallographic c-axis and X, Y in the basal plane. In phase III, the modes appearing in Y(ZZ)X, Y(ZY)X and Y(XY)X spectra belong to A, E_1 and E_2 species respectively (Hiraishi *et al* 1976). Of these A and E_1 species are also infrared active and therefore the modes belonging to these symmetries are expected

to show LO-TO splitting. Table 1 lists the frequencies observed at 296 K. The assignment of the modes is essentially similar to that given by Hiraishi *et al* (1976). However, there is one important difference *viz.* assignment of the $\nu_2^{E1(LO)}$ mode (Bansal *et al* 1981).

It is seen from figure 2 that external modes broaden over the temperature range 300 K—685 K (phase III) while the sulphate internal modes, more or less, remain unaffected as expected. The mode around 380 cm^{-1} (figure 2) which is likely to involve predominantly Li translation, spreads out considerably. The other features which emerge from figure 2 are that above T_c, in addition to external modes becoming heavily damped the internal modes $\nu_4(SO_4)$ and $\nu_3(SO_4)$ shift upwards in frequency by 28 cm^{-1} and 35 cm^{-1} respectively and also broaden remarkably. Further, intensity develops in the region ($\sim$465 cm^{-1}). Figures 3 and 4 confirm the sudden increase in widths for various internal modes. Also it is clear that unlike ν_4^A and ν_3^A there is no shift in the frequency for $\nu_4^{E_1}$, $\nu_4^{E_2}$, $\nu_3^{E_1}$ and $\nu_3^{E_2}$ modes across T_c.

Another observation of figures 3 is that in phase II the macroscopic field splitting for the $\nu_4^{E_1}$ mode is suppressed (see figure 6).

The intensity of the ν_1^A symmetric stretching mode in an off-diagonal geometry is shown in figure 5 as a function of temperature. The intensity is seen to steadily decrease upto a temperature of $\sim$450 K after which it stays practically constant. Above T_c it increases abruptly again. We discuss in the next section the nature of transformation from phase III to II in light of the above observations.

3. Analysis

Temperature variation of frequency and width of some selected modes are plotted in figures 6 and 7. It is evident that abrupt changes take place in the dynamics of the crystal across T_c.

In phase III, the triply degenerate ν_3 and ν_4 sulphate internal modes decompose into $A+B+E_1+E_2$ of which B is Raman inactive. From the results presented in the previous section it can be seen that

Table 1. Mode frequencies at 296 K and their assignments† in phase III.

		A(TO)	A(LO)	E_1(TO)	E_1(LO)	E_2
Internal modes	ν_1	1012	1012	—	—	—
	ν_2	—	—	466	445	467
	ν_3	1122	1201	1119	1200	1123
	ν_4	624	630	636	649	637
External modes		372[a]	*	408[a]	478[a]	404[a]
		202[b]	204[b]	41	44	131
		129	*			102
						50

†Of the total number of Raman active modes predicted from group theoretical analysis one external mode belonging to E_1 symmetry was not seen.
—Indicates that the internal mode has no component belonging to that symmetry.
*Indicates that the LO counterpart could not be observed.
[a]The mode involves predominantly lithium translation.
[b]This frequency is assigned to sulphate libration about the c-axis (ν_r).

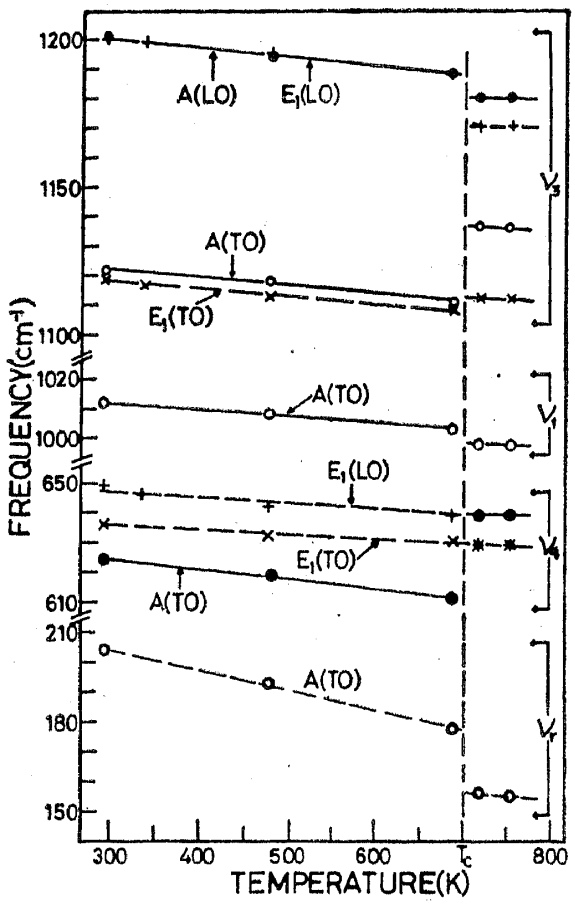

Figure 6. Mode frequency variation as a function of temperature. Lines are drawn through the points as guide to eye. ν_2 modes are omitted in this figure (see Bansal *et al* 1981).

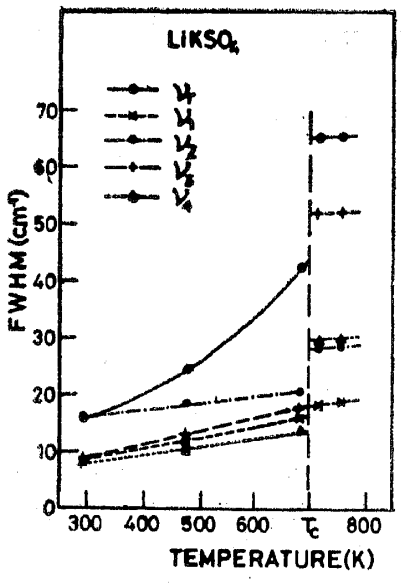

Figure 7. Line widths are plotted as a function of temperature. No correction for instrumental line width (3·5 cm^{-1}) has been applied.

(i) $\nu_i^{E_1}(SO_4) \sim \nu_i^{E_2}(SO_4)$, $i=2, 3, 4$ and

(ii) $\nu_i^{A}(SO_4) \sim \nu_i^{E_1}(SO_4)$; $\nu_i^{E_2}(SO_4)$, $i=3, 4$

The former implies small correlation splitting while the latter suggests near isotropy of crystalline field. However in phase II, crystal field anisotropy is strongly reflected in the frequency shift between the different components of $\nu_3(SO_4)$ (and also $\nu_4(SO_4)$) observed in ZZ and ZY polarizations (figures 2, 3).

Coming now to the ν_1 stretching mode (~ 1010 cm^{-1}) of SO_4 ion we note that the Raman tensor has a diagonal form

$$\begin{pmatrix} e & . & . \\ . & e & . \\ . & . & f \end{pmatrix}$$

where Z axis is taken along the crystallographic c-axis. For the scattering geometry shown in figure 5 (rotation of 45° about the x-axis) the tensor takes the following form:

$$\begin{pmatrix} e & . & . \\ . & \frac{1}{2}(e+f) & \frac{1}{2}(e-f) \\ . & \frac{1}{2}(e-f) & \frac{1}{2}(e+f) \end{pmatrix}$$

Therefore intensity in the Y'Z' polarization is a direct measure of anisotropy of the Raman polarizability tensor. The results presented in figure 5 show that the crystalline environment experienced by the sulphate ion becomes almost isotropic at around 450 K. It may be mentioned here that similar inference was drawn earlier on the basis of LO-TO splitting of the $\nu_2^{E_1}$ mode (Bansal *et al* 1981). Finally, above T_c there is an abrupt increase in peak intensity by a factor of ~ 6 which is again suggestive of strong anisotropy in phase II.

We next consider the types of disorder which may be present in the high temperature phase. Electrical conductivity of $LiKSO_4$ shows a sudden jump by about one order of magnitude at T_c (Ando 1962). This must be attributed to increased mobility of lithium ions. Every lithium atom has six other lithium atoms as its neighbours. Thermally generated vacancies are likely to induce Li to jump from site to site since the structure is very open and as noted earlier the Li 'translatory' modes broaden remarkably near T_c which is indicative of large amplitude motion. Positional disorder of Li would modify the crystalline environment of SO_4 ions to varying degree and is also likely to introduce disorder in the orientation of sulphate tetrahedra. These disorders are responsible for the abrupt increase in widths of the SO_4 internal modes. It is interesting to note here that sulphate internal modes in molten K_2SO_4-Li_2SO_4 mixtures show similar line shapes (Child *et al* 1980) particularly for the ν_3 mode. The suppression of LO counterparts of some of the internal modes may be linked to the disorder in SO_4 orientation as it will tend to quench the macroscopic field. The appearance of intensity in the ν_2 region in the (ZZ) polarization can also similarly be attributed to the destruction of three-fold symmetry element in phase II, which is believed to be orthorhombic (Chung and Hahn 1972). It may be pointed here that htis implies doubling of the unit cell volume. However, the fact that new lines or split-

ting of degenerate modes are not observed suggests that distortion from hexagonal symmetry is small.

Another experimental observation which may be mentioned here is that after the crystal is cycled through phase II, Raman intensity of certain lines in phase III undergoes considerable change. This is clearly seen in figure 8. Further, the optical activity, which is about 5°/mm (λ=4416 Å) for a crystal which has not been subjected to the heating and cooling cycle, drops to a much lower value after the thermal cycle. As we show in the next section, the above observations can be related to the appearance of domain structure.

4. Twinning in phase III

One can postulate different types of twins in phase III. The four distinct but energetically equivalent configurations are designated below as A, B, C and D.

A: The structure as shown in figure 1.

B: The structure obtained from A through the coordinate transformation $xyz \rightarrow yxz$ (coordinates are specified with respect to the crystallographic axes). This operation corresponds to the vertical mirror plane σ_v [$\bar{1}$10].

C: The structure obtained from A through the coordinate transformation $xyz \rightarrow xy\bar{z}$. This operation corresponds to the horizontal mirror plane σ_h [001].

D: The structure obtained from A through the coordinate transformation $xyz \rightarrow yx\bar{z}$. This operation corresponds to the 2-fold rotation axis C_2 [110].

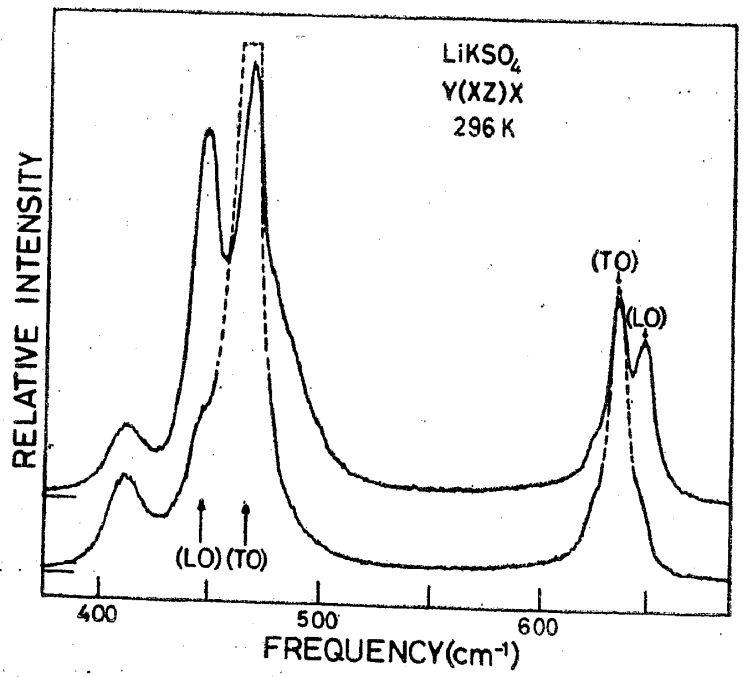

Figure 8. The lower trace corresponds to the spectra recorded from as grown crystal. In the Y(XZ)X geometry, TO components of ν_2 and ν_4 appear prominently. This may be contrasted with the spectra Y(ZY)X shown in figure 3 where LO modes are strong (Bansal *et al* 1980a). The upper trace is obtained when the specimen is heated above T_c and then cooled to room temperature. LO modes are now seen to pick up intensity.

Therefore the actual crystal can in principle be a combination of all the four types of domains. Expressed schematically it can be written as $p_1A + p_2B + p_3C + p_4D$ where $p_1 + p_2 + p_3 + p_4 = 1$. In a diffraction experiment one cannot distinguish between A and C (similarly between B and D). From the recent neutron and X-ray diffraction work* (Bhakay *et al* 1982) one gets $(p_1 + p_3) \simeq 0{\cdot}8$ and $(p_2 + p_4) \simeq 0{\cdot}2$.

In view of the above conclusion from diffraction experiments, we deemed it desirable to investigate if one can ascertain the presence of different domains in the sample from Raman data alone. The possibility of distinguishing different domains in a Raman experiment, basically involves examining the orientational relationship of different domains and then studying all the implications for scattering experiments in different configurations. A straightforward calculation using transformation law for Raman polarizability tensors shows that only with respect to polar (E_1) modes is there any distinction possible.

In particular, the intensities for the $E_1(TO)$ modes (Bansal *et al* 1980a) in the Y(XZ)X and Y(ZY)X configurations (referred to the laboratory fixed frame) for the different domains are given by

$$I^A_{XZ}(TO) = I^B_{ZY}(TO) = I^C_{XZ}(TO) = I^D_{ZY}(TO) = (c + d)^2$$

$$I^A_{ZY}(TO) = I^B_{XZ}(TO) = I^C_{ZY}(TO) = I^D_{XZ}(TO) = (c - d)^2$$

where c and d are elements of the Raman polarizability tensor (Bansal *et al* 1980a) corresponding to the crystal domain A. In this sense a possibility exists of distinguishing the domains (A, C) *vis-a-vis* (B, D). (No distinction is possible between A and C or between B and D.) Although one cannot unambiguously estimate *quantitatively* the relative amounts of (A, C) and (B, D), some limits can be established. From our Raman intensity measurements of the ν_2 mode we find that $(p_2 + p_4) \leqslant 0{\cdot}06$. The discrepancy between Raman and neutron results suggests that twinned domains may coexist in different proportions in different specimens.

We now turn to figure 8. The results presented here show that twins of type B (or D) appear in the specimen when it is subjected to thermal cycling. The variation of optical activity is also easily understood because the sense of optical rotation is opposite in the domains A and B. The existence of orientational disorder postulated in phase II is consistent with the appearance of twins of type B (and D) after thermal cycling as the sulphate orientational disorder can lead to growth of domains on cooling in which SO_4 tetrahedra are reoriented differently.

The underlying feature of the twin domains which may be noted here is that transformation from one to the other essentially involves reorientation of SO_4 tetrahedra. For example A → B is associated with reorientation of SO_4 by 60° about the S-O(1) and while A → C (and D) corresponds to reorientation by 180° about an axis which lies in the plane defined by the three remaining oxygen atoms (O(2)).

It may be remarked here that reorientation of the tetrahedral ion is intimately connected with appearance of twin domains in K_2SeO_4 and other related compounds also (Sawada *et al* 1976; Shiozaki *et al* 1977).

*The other finding of the authors is that the crystal displays only a pseudohexagonal symmetry in phase III. However, Raman data do not indicate any departure from hexagonal symmetry (C_6).

5. Discussion

The Raman scattering studies described in earlier sections show that there is an abrupt change of frequency and width of external and internal modes across the phase transition III-II. Lattice constant (Fischmeister and Ronnquist 1960), thermal expansion coefficient (Sharma 1979) and dielectric constant (Ando 1962) also exhibit discontinuous changes at T_c. The heat of transition has been found to be $1{\cdot}6 \pm 0{\cdot}2$ kcal/mole with a hysteresis of about 15° (Rao 1981). These establish the transition as first order.

If symmetry of the 'prototype' phase (phase I) is taken as 6/mmm then it can be shown (Aizu 1969) that $LiKSO_4$ in phase III ($P6_3$) can only be ferroelectric. Experimentally $LiKSO_4$ has been found to be pyroelectric in phase III (Ando 1962), but ferroelectricity could not be established. This is not surprising because reversal of polarization would imply reorientation of sulphate tetrahedra in the unit cell which has to occur against a large potential-well. However, as mentioned earlier (§ 4) domains with opposite polarization do appear when the crystal is cycled through phase II. In conclusion we note that reorientation of the sulphate ion plays a fundamental role in the transformation of $LiKSO_4$ to various phases.

Acknowledgements

The authors wish to thank Dr A Sequeira and Dr V K Wadhawan for useful discussions. They are also thankful to Shri P S Parvathanathan for carrying out DSC measurements. The authors are grateful to Dr P K Iyengar and Dr N S Satya Murthy for their interest in this work.

References

Aizu K 1969 *J. Phys. Soc. Jpn.* **27** 387
Ando R 1962 *J Phys. Soc. Jpn.* **17** 937
Bansal M L, Deb S K, Roy A P and Sahni V C 1979 *Nucl. Phys. Solid State Phys.* **C22** 365
Bansal M L, Deb S K, Roy A P and Sahni V C 1980 a *Solid State Commun.* **36** 1047
Bansal M L, Deb S K, Roy A P and Sahni V C 1980b *Nucl. Phys. Solid State Phys.* **C23** 621
Bansal M L, Deb S K, Roy A P and Sahni V C 1981 *J. Physique* **C6** Suppl. 12 902
Bhakey-Tamhane S, Sequeira A and Chidambaram R 1981a *Acta Cryst.* **A37** (Suppl.) C108
Bhakay-Tamhane S 1981b Private communication
Bhakay-Tamhane S, Sequeira A and Chidambaram R 1982 (to be published)
Breczewski T, Krajewski T and Mroz B 1981 *Ferroelectrics* **33** 9
Child W C, Smith D H and Begun G M 1980 *Proc. VIIth Int. Conf. Raman Spectroscopy*, (Ed) W F Murphy (Amsterdam: N H Publ. Co.) p. 268
Chung S J and Hahn T 1972 *Acta Cryst.* **A28** 557
Fischmeister H F and Ronnquist A 1960 *Arkiv Kemi* **15** 393
Hiraishi J, Taniguchi N and Takahashi H 1976 *J. Chem. Phys.* **65** 3821
Madhu B R and Narayanan P S 1981 *Nucl. Phys. Solid State Phys.* **C24** 335
Mathieu J P, Couture L and Poulet H 1955 *J. Phys. Rad.* **16** 781
Ranga Prasad T, Venudhar Y C, Leela Iyengar and Krishna Rao K V 1978 *Pramana* **11** 81
Rao U R K 1981 Private communication
Sawada A, Makita Y and Takagi Y 1976 *J. Phys. Soc. Jpn.* **41** 174
Sharma D P 1979 *Pramana* **13** 223
Shiozaki S, Sawada A, Ishibashi X and Takagi Y 1977 *J. Phys. Soc. Jpn.* **43** 1314
Wyckoff R W G 1965 *Crystal Structures* (New York: Interscience) Vol. 3